Spoofing PRNU Patterns of Iris Sensors while Preserving Iris Recognition

Sudipta Banerjee, Vahid Mirjalili, Arun Ross Department of Computer Science and Engineering Michigan State University

{banerj24, mirjalil, rossarun}@cse.msu.edu

Abstract

The principle of Photo Response Non-Uniformity (PRNU) is used to link an image with its source, i.e., the sensor that produced it. In this work, we investigate if it is possible to modify an iris image acquired using one sensor in order to spoof the PRNU noise pattern of a different sensor. In this regard, we develop an image perturbation routine that iteratively modifies blocks of pixels in the original iris image such that its PRNU pattern approaches that of a target sensor. Experiments indicate the efficacy of the proposed perturbation method in spoofing PRNU patterns present in an iris image whilst still retaining its biometric content.

1. Introduction

The process of automatically determining the sensor that produced a given image is referred to as *sensor identification*. While a number of sensor identification methods have been discussed in the literature [35, 20, 9], the ones based on Photo Response Non-Uniformity (PRNU) [32, 11, 18] have gained prominence in the recent literature. PRNU refers to the non-uniform response of individual pixels across the sensor array to the same illumination as a consequence of manufacturing defects introduced during sensor production. PRNU manifests itself as a noise pattern in the images generated by a sensor. This noise pattern is believed to be unique to every sensor [17]. A number of schemes have been designed to compute the PRNU noise of a sensor based on the images generated by it [7].

More recently, the principle of PRNU has been used to perform sensor identification in the context of iris biometrics by processing the near-infrared (NIR) ocular images acquired by typical iris sensors [37, 24, 14, 12, 13, 8, 33]. In this case, sensor identification (or device identification) can be used in conjunction with biometric recognition to authenticate both the identity of a device (e.g., a smartphone) as well as the individual using the device [19].

Given the forensic value of PRNU in determining the

origin of an image (i.e., the sensor or device that produced it), we explore if it is possible to alter an image such that its source, as assessed by a PRNU estimation scheme, is confounded. We impose two constraints:

- The modified image must spoof the PRNU pattern of a pre-specified target sensor.
- The biometric utility of the modified image must be retained, viz., the modified ocular image must match successfully with the original image.

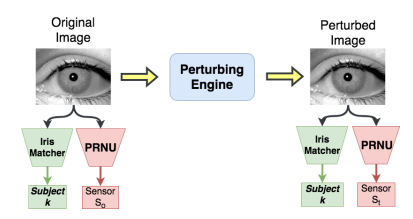


Figure 1. The objective of this work is to perturb an ocular (iris) image such that its PRNU pattern is modified to spoof that of another sensor, while not adversely impacting its biometric utility.

This kind of attack can be considered as a 'targeted attack', since the sensor whose PRNU pattern has to be spoofed is pre-specified. In the literature, it is also referred to as fingerprint-copy attack [22, 37], because the objective is to copy the sensor pattern or 'fingerprint' corresponding to the target sensor to an image acquired using a different source sensor.

The proposed work has two distinct benefits. Firstly, it allows us to assess the feasibility of PRNU spoofing from a counter-forensic perspective. The widespread use of forensic techniques for examining the validity and origin of digital media [21, 27] necessitates the study of attacks that can potentially undermine the performance of such forensic methods. For example, an adversary may maliciously attempt to link an image to a different camera in an effort to mislead law enforcement investigators [22]. Secondly, establishing the viability of such spoof attacks would promote the development of more robust PRNU estimation schemes [33]. Figure 1 summarizes the objective of this

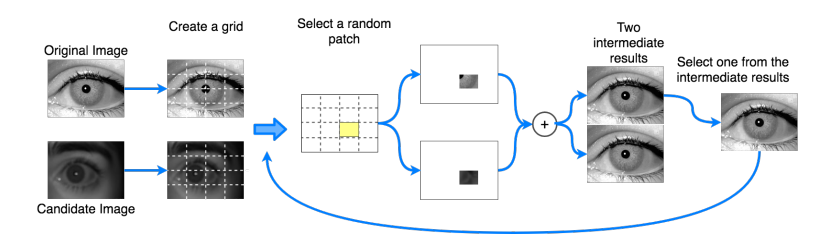


Figure 2. The proposed algorithm for deriving perturbations for the input image using the candidate image.

work.

The remainder of the paper is organized as follows. Section 2 briefly reviews the PRNU based sensor identification scheme used in this work. Section 3 presents methods that have been described in the literature for sensor anonymization and spoofing. Section 4 describes the proposed method for spoofing PRNU patterns. Section 5 provides details about the datasets used, the experimental protocols employed, and reports the results obtained using the proposed method. Section 6 summarizes the paper and indicates future work.

2. Photo Response Non-Unformity (PRNU)

PRNU estimation entails computing the reference pattern of a sensor based on a set of training images acquired using the sensor. This reference pattern is then used by a sensor classifier to identify the sensor that was used to acquire a given test image. This is accomplished by correlating the reference pattern of the sensor with the noise residual of the test image to compute a correlation score. The image is assigned to the sensor whose reference pattern yields the highest correlation value. Here, we used Normalized Cross-Correlation (NCC) for computing the correlation score [12, 8]. PRNU estimation can be done using numerous approaches [32, 28, 25, 31, 30, 7]. In this work, we used the Maximum Likelihood Estimation (MLE) based PRNU estimation scheme [11], which has been demonstrated to suppress image artifacts not associated with the sensor-specific pattern and has resulted in very good performance [14, 12].

MLE based PRNU estimation uses a weighted averaging of the noise residuals extracted from a set of training images pertaining to the sensor; each noise residual is weighted by its corresponding training image, to derive the maximum-likelihood estimate of the reference pattern. Wiener filtering and zero-mean operations are applied to the noise residuals to address interpolation artifacts arising due to the Bayer pattern. In our experiments, L_2 -normalization of the test noise residual is performed to account for the variations in the PRNU strength of different sensors [26]. The MLE of the reference pattern corresponding to a sensor is computed as, $\hat{K} = \frac{\sum_{i=1}^{N} w_i I_i}{\sum_{i=1}^{N} I_i^2}$. Here, w_i is the noise residual

obtained using a wavelet-based denoising filter applied to training image I_i and $w_i = I_i - F(I_i)$, where, F denotes the Daubechies Quadrature Mirror Filter [32].

3. Perturbing PRNU Pattern

The counter-forensics literature describes techniques that can be used to suppress or perturb the PRNU pattern embedded in an image. This is often referred to as source anonymization [16], i.e., obscuring the "fingerprint" of the source sensor in an image so as to anonymize the origin of the image. Source anonymization can be used as a privacy preservation scheme, particularly relevant when the sensorspecific details can be used to associate a sensor with its owner. Assuming that each device is typically associated with a single user, device identification can be indirectly used to reveal the identity of the person possessing that specific device. There have been primarily two approaches to perturb the PRNU pattern for this purpose, namely, (i) compression and filtering based schemes: typically involves the use of strong filtering schemes such as, flat-field subtraction [38] or Wiener filtering [10] which can degrade the PRNU pattern leading to incorrect source attribution, and (ii) geometric perturbation based schemes: example includes 'seam carving' [15, 10] which distorts the alignment between the sensor reference pattern and the test noise residual, impeding the process of correlating the reference pattern with the test noise residual.

In contrast to source anonymization, *PRNU spoofing* not only suppresses the fingerprint of the source sensor, but it also inserts the fingerprint of the target sensor. An adversary may tamper with the digital evidence (within the chain of custody) to maliciously exculpate a guilty person or worse, incriminate an innocent person. PRNU spoofing can be achieved either by PRNU injection, or, through PRNU substitution. The first method adds the weighted reference pattern of a pre-selected target sensor to the input image, I [22]. The modified image becomes $I' = [I + I \times \gamma \hat{K}_T]$. Here, \hat{K}_T is the reference pattern of the target sensor T. The term γ was set to 1 for sake of convenience (in our implementation of the algorithm). The second method subtracts the PRNU pattern of the source sensor in an image and then adds the PRNU pattern of a target sensor [29]. The

modified image is represented as $I' = I - \gamma \hat{K}_S + \beta \hat{K}_T$. I belongs to the source sensor S, whose reference pattern is \hat{K}_S . The terms γ and β are positive scalars and are set to 1. In [37] the authors examine the validity of the PRNU spoofing in the context of iris sensors using PRNU injection [23], where the forged image is computed as $I' = [F(I) + \gamma \hat{K}_T]$. Here, $F(\cdot)$ is the wavelet based denoising filter discussed in Section 2. The authors further performed triangle test to detect the spoof attack, but did not analyze the impact of the PRNU spoofing on iris recognition performance.

In this paper, our objective is to perform PRNU spoofing in a principled manner, which obviates empirically tuned factors such as γ,β above and works for any arbitrary pair of source and target iris sensors. In addition, we wish to retain the biometric utility of the PRNU-spoofed image. The proposed method offers a strong motivation for the adversary; the intruder requires minimal knowledge about PRNU estimation schemes (generation of sensor reference pattern and computation of scalar parameters), he/she can perturb the images directly to perform PRNU spoofing.

4. Proposed method

In this section, we formally describe the objective and the method used to address this objective.

4.1. Problem formulation

Let X denote an NIR image of width w and height h obtained from sensor $S \in \{S_1, S_2, ..., S_n\}$. We assume that we are given a PRNU-based sensor classifier, ϕ , where $\phi_i(X)$ determines the probability that image X is associated with sensor S_i . Then, the sensor label for an input NIR image Xcan be predicted using $\arg \max\{\phi_i(X)\}$. Furthermore, we are given a biometric iris matcher, M, where $M(X_1, X_2)$ determines the match score between two input samples X_1 and X_2 . Given an input iris image, X, and iris matcher, M, our goal is to devise a perturbation engine Ψ that can modify the input image as $Y = \Psi(X)$ such that the PRNU-based sensor classifier ϕ will *not* predict the correct sensor label of the perturbed image Y, while the iris matcher, M, will successfully match Y with X. As a result, the match score between a pair of perturbed images $[M(Y_1, Y_2)]$ as well as that of a perturbed sample with an original sample, $[M(X_1, Y_2)]$ and $[M(Y_1, X_2)]$, are expected to be similar to the match scores between the original samples $[M(X_1, X_2)]$. The steps used to achieve this task is described next.

4.2. Deriving perturbations

Given a single image X from the source sensor S_o , a gallery of images $G_{S_t} = \{X_1,...,X_L\}$ from the target sensor S_t , and a set of K random patch locations $P = \{p_1,...,p_K\}$, we first select a candidate image, X_c , where $c \in [1,\cdots,L]$, from the gallery to perturb the input image.

The objective is mainly to preserve the structural similarity between the perturbed output image Y and the original image X. Thus, X_c , merely guides the "direction" in which X has to be perturbed. In order to accomplish this goal, we develop the routine described below.

Determination of the candidate image:

Step I: For the input image X, first compute the average pixel intensity in each patch $p_k \in P$ to obtain a vector \mathbf{v}_X (of size K). In our experiments, K = 10 and each patch is of size 10×10 .

Step II: Repeat the above step for each of the gallery images to obtain a set of vectors \mathbf{v}_{g_i} , where, $i = 1, \dots, L$. The value of L depends on the number of test images in the datasets (see Table 1).

Step III: Next, compute the correlation between \mathbf{v}_X and \mathbf{v}_{g_i} corresponding to each gallery image to obtain a set of L correlation scores.

Step IV: The gallery image producing the highest correlation score is selected as the candidate image (X_c) for the given input image (X). Thus, $X_c = X_{mc}$ where $mc = \underset{i \in [1, \cdots, L]}{\operatorname{arg}} \max \{Corr(\mathbf{v}_X, \mathbf{v}_{g_i})\}.$

After obtaining the candidate image X_c from the gallery of the target sensor S_t , the perturbations for image X are then derived with the help of X_c . First, we create a grid of non-overlapping patches of size $h_p \times w_p$ on both the images X and X_c . Next, we construct a mask matrix Mask, such that Mask[i,j]=1 if $\left(\lfloor\frac{i}{h_p}\rfloor,\lfloor\frac{j}{w_p}\rfloor\right)=(p_x,p_y)$, and Mask[i,j] is zero elsewhere. Then, the image X is perturbed iteratively as described below.

Spoofing PRNU pattern:

Step I: First, we select a random patch from the grid, and then update the pixels inside this patch along two vector directions, namely the i) positive direction and the ii) negative direction [34].

Step II: Next, create a perturbed image in the positive direction $Y^u = Y^{(iter)} + \alpha Mask \odot (Y^{(iter)} - X_c)$; and another perturbed image in the negative direction $Y^v = Y^{(iter)} - \alpha Mask \odot (Y^{(iter)} - X_c)$. In both directions, we set α to 0.01.

Step III: Correlate Y^u and Y^v with the target reference pattern, to compute $Corr(Y^u, S_t)$ and $Corr(Y^v, S_t)$, respectively. Note, $Corr(\cdot, \cdot)$ computes NCC.

Step IV: For the current iteration, check if $Corr(Y^u, S_t) > Corr(Y^v, S_t)$, then assign perturbed image $Y^{(iter)} = Y^u$ else, set $Y^{(iter)} = Y^v$. Increment iter by 1.

Step V: Repeat Steps I - IV until iter > 3000 or, the relative difference between the NCC values exceeds a certain threshold, $\eta = 0.1$, i.e., $\frac{Corr(Y^{(iter)}, S_t) - Corr(Y^{(iter)}, S_o)}{Corr(X, S_o)} > \eta.$

At the end of the routine the perturbed image will be incorrectly attributed by the sensor classifier to S_t . The steps

Table 1. Specifications of the datasets used in this work.

Dataset	Sensor Name (Abbreviation)	Image Size	Number of Images Used (Training set+Testing set)	Number of Subjects
BioCOP 2009 Set I	Aoptix Insight (Aop)	640×480	995 (55+940)	100
IITD [4]	Jiristech JPC 1000 (JPC)	320×240	995 (55+940)	100
CASIAv2 Device2 [1]	CASIA-IrisCamV2 (IC)	640×480	995 (55+940)	50
IIITD Multi-spectral Periocular (NIR subset) [3]	Cogent (Cog)	640×480	588 (55+533)	62
ND CrossSensor Iris 2013 Set II [6]	LG 4000 (LG40)	640×480	615 (55+560)	99
MMU2 [5]	Panasonic BM-ET 100US Authenticam (Pan)	320×238	55 (55+0)	6
ND Cosmetic Contact Lens 2013 [6]	IrisGuard IG AD100 (AD)	640×480	55 (55+0)	4
WVU Off-Axis	EverFocus Monochrome CCD (Ever) [36]	640×480	55 (55+0)	7
CASIAv2 Device 1 [1]	OKI IrisPass-h (OKI)	640×480	55 (55+0)	3
CASIAv4-Iris Thousand subset [2]	IrisKing IKEMB100 (IK)	640×480	55 (55+0)	3
ND CrossSensor Iris 2013 Set I [6]	LG 2200 (LG22)	640×480	55 (55+0)	5

Table 2. Confusion matrix for sensor identification involving unperturbed but resized images. The test noise residuals of images from 5 sensors are compared against reference patterns from 11 sensors. The last column indicates sensor identification accuracy.

	Aop	JPC	IC	Cog	LG 40	Pan	AD	Ever	OKI	IK	LG 22	Accuracy (%)
Aop	900	1	2	1	9	4	3	3	9	7	1	95.74
JPC	2	919	4	2	5	0	0	4	1	2	1	97.77
IC	0	0	940	0	0	0	0	0	0	0	0	100
Cog	2	1	2	546	2	0	2	0	0	5	0	97.51
LG40	0	0	0	0	529	0	0	3	1	0	0	99.25

of the PRNU spoofing algorithm are illustrated in Figure 2.

5. Experiments and Results

In this section, we describe the datasets and sensors employed in this work, followed by the experiments conducted on the datasets. Results are reported and analyzed in the context of PRNU spoofing and iris recognition.

5.1. Datasets

In this work, experiments are conducted using 11 different sensors from 11 iris datasets. The PRNU spoofing process typically involves a single source sensor and a single target sensor from the set of 11 sensors. Thus there can be a total of $^{11}P_2=110$ combinations for PRNU spoofing. However, for the sake of brevity, we performed 20 different PRNU spoofing experiments involving 5 sensors. The sensor details and image specifications of the 11 sensors are described in Table 1. PRNU spoofing entails 5 source sensors $\{Aop, JPC, IC, Cog, LG40\}$, and for each source sensor, the remaining 4 sensors serve as target sensors, thus resulting in 20 different PRNU spoofing experiments.

5.2. Sensor identification before PRNU spoofing

Due to the variations in the sizes of the images belonging to the source and the target sensors, all the images were resized to a fixed spatial resolution of 160×120 to facilitate the PRNU spoofing process. We then evaluated the sensor identification accuracy based on these resized images prior to PRNU spoofing. The sensor identification involves deriving sensor reference patterns using 55 training images from each of the 11 sensors, followed by extraction of test noise residuals belonging to the 5 sensors, and finally correlat-

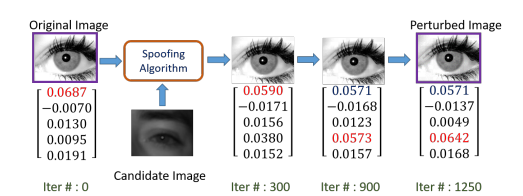


Figure 3. Illustration of perturbed images generated iteratively for the case of an image from the Aoptix (S_o) sensor perturbed using the candidate image belonging to Cogent (S_t) . For the sake of brevity, NCC values corresponding to the first 5 sensors in Table 1 are mentioned in the figure.

ing them. The subjects in the training set and the test set are disjoint. The sensor identification accuracy and the corresponding confusion matrix is presented in Table 2. The results indicate accurate sensor identification using MLE PRNU scheme. Next, we describe the experiments and results pertaining to the PRNU spoofing process.

5.3. Sensor identification after PRNU spoofing

The PRNU spoofing process involves perturbing the original image from a source sensor using a candidate image belonging to the target sensor, whose PRNU needs to be spoofed. The impact of the perturbations on spoofing the PRNU pattern has been reported in terms of *Spoof Success Rate* (SSR), which computes the proportion of test images classified as belonging to the target sensor. The results of spoofing are presented in Table 3.

We implemented the PRNU substitution algorithm [29], referred to as Baseline 1 algorithm, and the fingerprint-copy technique [22], referred to as Baseline 2 algorithm for comparison. Baseline 1 is implemented following normalization of the source and target reference patterns with respect to the maximum of the two. The normalization is required to account for the variation in the PRNU strength associated with different sensors. Baseline 2 algorithm is implemented exactly as described in Section 3.

Results indicate that 15 out of 20 times, the proposed algorithm outperforms Baseline 1 technique and performs considerably better than Baseline 2 method, 16 out of 20 times. We believe that the value of the factors γ and β play a significant role for the success of both the baseline meth-

Table 3. Results of PRNU spoofing for each of the 5 sensors, namely, Aop, JPC, IC, Cog and LG40 sensors (along the first column) using images from 4 sensors (along the second column). The test noise residual after the perturbation process is compared against the reference patterns of 11 sensors (see Table 1). The last 3 columns indicate the proportion of the perturbed images successfully classified as belonging to the target sensor and is denoted as the Spoof Success Rate (SSR). The highest values are bolded.

Original	Target	Communication of the Land Department of the L										SSR (%) for	SSR (%) for	SSR (%) for	
Sensor	Sensor	Sensor classes compared against perturbed PRNU										Baseline 1	Baseline 2	proposed method	
Aop		Aop	JPC	IC	Cog	LG40	Pan	AD	Ever	OKI	IK	LG22			
	IC	21	0	891	0	6	2	1	5	6	5	3	92.77	13.51	94.79
	JPC	4	894	3	3	8	2	2	2	9	12	1	92.55	67.98	95.11
	Cog	7	2	3	890	7	5	2	2	13	5	4	79.89	0.21	94.68
	LG40	66	4	4	4	836	3	0	4	7	8	4	79.15	10.00	88.94
JPC	Aop	905	18	3	3	4	0	0	2	2	2	1	49.15	1.91	96.28
	IC	2	209	712	2	4	2	1	3	2	2	1	99.79	100	75.74
	Cog	3	94	4	817	5	5	0	5	2	1	4	35.53	0.21	86.91
	LG40	1	61	3	1	861	5	0	3	1	2	2	8.09	9.26	91.60
	Aop	910	0	30	0	0	0	0	0	0	0	0	48.72	0	96.81
IC	JPC	0	797	143	0	0	0	0	0	0	0	0	100	53.09	84.79
IC	Cog	0	0	243	697	0	0	0	0	0	0	0	46.70	0	74.15
	LG40	0	0	46	0	894	0	0	0	0	0	0	1.91	0.11	95.11
Cog	Aop	552	0	0	0	2	0	2	0	0	4	0	100	38.57	98.57
	JPC	1	546	0	0	1	0	2	2	0	8	0	100	100	97.50
	IC	2	0	545	2	2	0	2	0	1	5	1	100	100	97.32
	LG40	1	0	0	0	550	0	2	1	0	6	0	82.32	35.00	98.21
LG40	Aop	330	0	3	0	198	0	0	0	1	1	0	9.94	1.31	61.91
	JPC	0	491	0	0	38	0	0	2	1	1	0	9.38	24.20	92.12
	IC	0	0	393	0	136	0	0	3	1	0	0	11.44	99.44	73.73
	Cog	0	0	0	479	50	0	0	2	1	1	0	4.69	0.19	89.87

ods and is sensor-specific. With regards to the proposed algorithm, the PRNU is successfully spoofed in most of the cases barring the case where the target sensor is Aoptix and the source sensor is LG 4000 (\approx 62% SSR). Inspection of the images acquired using LG 4000 sensor reveals the presence of image padding, which may make the PRNU spoofing process difficult. We hypothesize that the perturbation algorithm may require more number of iterations to achieve the desired threshold η . Figure 3 shows an input image undergoing iterative perturbations. The original (unperturbed) image belongs to the Aoptix sensor and is perturbed using a candidate image from the target sensor, Cogent. The subsequent shift of the NCC values from being highest for the source sensor (Aoptix) to being highest for the target sensor (Cogent), indicates the success of the proposed method.

The average number of iterations required for successful PRNU spoofing varied between 200 to 2200. An experiment is further conducted to study the impact of increasing the number of iterations on the proposed PRNU spoofing process. This experiment is conducted for the specific case where the source sensor is LG 4000 and the target to be spoofed is the Aoptix sensor. The reason for selecting this pair is due to the poor SSR reported for this specific set of sensors (see the fifth block in Table 3). We speculate that with an increase in the number of iterations, the PRNU spoofing process may become successful and improve the SSR as a result. In this regard, the new experimental set-up had the maximum number of iterations set to 6000 (twice the earlier terminating criterion). As a result, the SSR increased considerably from 61.91% to 79.73%, i.e., a $\approx 20\%$ increase was observed. 425 out of 533 test images belonging to the LG 4000 sensor were successfully classified as originating from the Aoptix sensor when the number of iterations was increased.

5.4. Retaining biometric matching utility

The impact of the perturbations on iris recognition performance is evaluated next using the VeriEye iris matcher. We designed three experiments for analyzing biometric matching performance. First, the match scores between all pairs of iris samples before perturbation were computed. In the second experiment, we computed the match scores between all pairs of perturbed samples. In the third experiment, we computed match scores between all iris samples before perturbation and all samples after perturbation. This is referred to as the cross-matching scenario. In the third set of experiments, the genuine scores are computed by employing 2 sample images (from the same subject), one sample belonging to the set of unperturbed images and the other sample from the set of perturbed images. The impostor scores are generated by pairing samples belonging to different subjects; one image is taken from the set of unperturbed images, while the other is taken from the set of perturbed

Figure 4 shows the ROC curves obtained from these three experiments for each set of perturbations. The ROC curves confirm that the perturbed images do not negatively impact the matching utility. In all cases, the ROC curves from perturbed images are within 1% variation from the ROC curve of the original samples before perturbations, except for the IrisCam (IC) sensor. Further, we note that the matching performance of samples from the Cogent (Cog) sensor is extremely degraded. However, we believe the reason for this degradation in performance is due to the low quality of the original images due to illumination variations. Yet, perturbations have not further deteriorated the match-

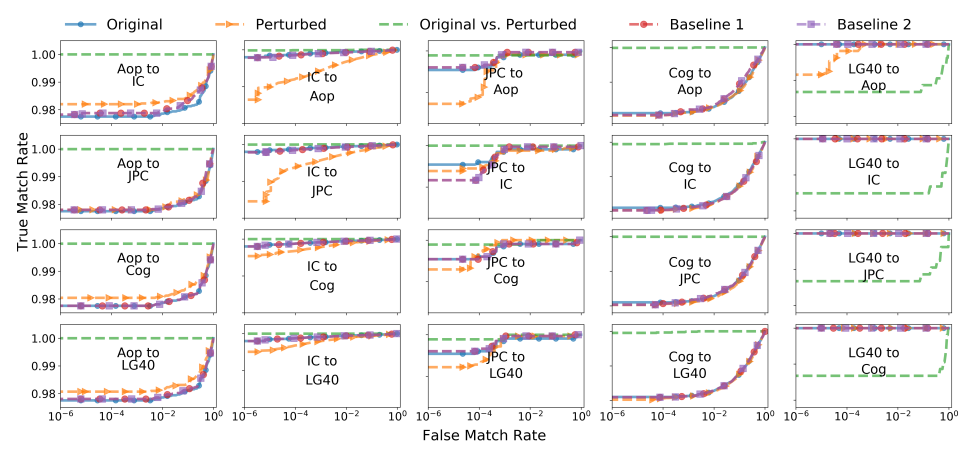


Figure 4. ROC curves of matching performance obtained using the VeriEye iris matcher software. The terms 'Original', 'Perturbed' and 'Original vs. Perturbed' indicate the three different matching scenarios (see Section 5.4). 'Original' indicates matching only unperturbed images; 'Perturbed' indicates matching only perturbed images; 'Original vs. Perturbed' indicates the cross-matching case where unperturbed images are matched against perturbed images. Note that the curves obtained from perturbed images match very closely with the curves corresponding to the unperturbed images illustrating preservation of iris recognition for each sensor depicted in each column. The results are compared with Baseline 1 and 2 algorithms discussed in Section 5.3.



Figure 5. Example of PRNU spoofed images originating from the JPC 1000 sensor (first column) is illustrated for Baseline 1 (second column), Baseline 2 (third column) and the proposed method (last column). Here, the target sensor is Aoptix.

ing performance, as evidenced by the ROC curves before and after perturbations that are very similar to each other. In addition, the iris recognition performance following PRNU spoofing using the baseline algorithms is analyzed. The results indicate that the proposed method is comparable with the baseline algorithms in terms of iris recognition performance. Furthermore, we have analyzed the matching performance involving LG 4000 as the source sensor and Aoptix as the target sensor with increased number of iterations. The result confirms that increasing the number of iterations which improves the SSR, does not degrade the matching performance.

In summary, the following important observations in the context of both PRNU spoofing and iris recognition preservation can be made.

i) The PRNU pattern of a sensor can be successfully spoofed by *directly* modifying an input image, without invoking the sensor reference pattern of the target sensor. This enforces the fact that PRNU is dependent on pixel intensities and begs the question *Is there a generalized way to capture the Sensor Pattern Noise free from pixel intensity influences?* Experiments are conducted using 11 iris sensors and the PRNU spoofing process is demonstrated using

5 sensors and compared with existing approaches. Results show that the proposed method performs substantially better than the baseline algorithms in a majority of the cases. Visual inspection reveals comparable results with the baseline algorithm as illustrated in Figure 5.

ii) The iris recognition performance is retained within 1% of the original, with the exception of images from the IrisCam (IC) sensor, where the degradation in performance (crossmatching scenario) is around 10% when the target sensors are Aoptix (Aop) and JPC 1000 (JPC). However, it should be noted that the iris recognition performance using perturbed images *only*, is comparable to the performance involving the unperturbed images (also when compared with the baseline algorithms).

6. Summary and Future Work

In this work, we demonstrate the potential of PRNU spoofing, while preserving the biometric recognition performance in the context of NIR ocular images. In the proposed strategy, a test image belonging to a particular sensor is modified iteratively using patches from a candidate image belonging to a target sensor, whose PRNU is to be spoofed. We examine the impact of these perturbations on PRNU spoofing as well as iris recognition performance. Experiments are conducted in this regard using 11 sensors and compared with two existing PRNU spoofing algorithms. Results show the perturbations using the proposed method can successfully spoof the PRNU pattern of a target sensor, but do not significantly degrade the iris recognition performance in a majority of the cases.

Future work will involve performing the proposed PRNU spoofing process on a larger set of sensors. Fi-

nally, we will look into developing new sensor identification schemes that are resilient to spoof attacks.

References

- [1] CASIA Iris Version 2 database. http://biometrics.idealtest.org/dbDetailForUser.do?id=2. [Online: accessed 10-July-2018].
- [2] CASIA Iris Version 4 Thousand database. http://biometrics.idealtest.org/dbDetailForUser.do?id=4. [Online: accessed 10-July-2018].
- [3] IIITD Multispectral Periocular database NIR subset. http://www.iab-rubric.org/resources/ impdatabase.html. [Online: accessed 10-July-2018].
- [4] IITD database. http://www4.comp.polyu.edu.hk/ ~csajaykr/IITD/Database_Iris.htm. [Online: accessed 10-July-2018].
- [5] MMU2 database. http://www.cs.princeton.edu/ ~andyz/irisrecognition. [Online: accessed 10-July-2018].
- [6] ND Cross Sensor and Cosmetic Contact Lenses databases. https://sites.google.com/a/nd.edu/ public-cvrl/data-sets. [Online: accessed 10-July-2018].
- [7] M. Al-Ani and F. Khelifi. On the SPN estimation in image forensics: A systematic empirical evaluation. *IEEE Trans*actions on Information Forensics and Security, 12(5):1067– 1081, May 2017.
- [8] S. Banerjee and A. Ross. From image to sensor: Comparative evaluation of multiple PRNU estimation schemes for identifying sensors from NIR iris images. In *Fifth International Workshop on Biometrics and Forensics*, 2017.
- [9] S. Bayram, H. Sencar, N. Memon, and I. Avcibas. Source camera identification based on CFA interpolation. In *IEEE International Conference on Image Processing*, volume 3, pages III–69–72, Sept 2005.
- [10] S. Bayram, H. T. Sencar, and N. D. Memon. Seam-carving based anonymization against image and video source attribution. In *IEEE 15th International Workshop on Multimedia Signal Processing (MMSP)*, pages 272–277, Sept 2013.
- [11] M. Chen, J. Fridrich, M. Goljan, and J. Lukas. Determining image origin and integrity using sensor noise. *IEEE Transactions on Information Forensics and Security*, 3(1):74–90, March 2008.
- [12] L. Debiasi and A. Uhl. Techniques for a forensic analysis of the CASIA-IRIS V4 database. In 3rd International Workshop on Biometrics and Forensics (IWBF), pages 1–6, March 2015.
- [13] L. Debiasi and A. Uhl. Comparison of PRNU enhancement techniques to generate PRNU fingerprints for biometric source sensor attribution. In 4th International Workshop on Biometrics and Forensics (IWBF), pages 1–6, March 2016.
- [14] L. Debiasi, A. Uhl, and Z. Sun. Generation of iris sensor PRNU fingerprints from uncorrelated data. In 2nd International Workshop on Biometrics and Forensics, pages 1–6, March 2014.

- [15] A. E. Dirik and A. Karaküçük. Forensic use of photo response non-uniformity of imaging sensors and a counter method. Opt. Express, 22(1):470–482, Jan 2014.
- [16] A. E. Dirik, H. T. Sencar, and N. Memon. Analysis of seam-carving-based anonymization of images against PRNU noise pattern-based source attribution. *IEEE Transactions on Information Forensics and Security*, 9(12):2277–2290, Dec 2014.
- [17] T. Filler, J. Fridrich, and M. Goljan. Using sensor pattern noise for camera model identification. *15th IEEE International Conference on Image Processing*, pages 1296–1299, Oct 2008.
- [18] J. Fridrich. Digital image forensics. IEEE Signal Processing Magazine, 26(2):26–37, March 2009.
- [19] C. Galdi, M. Nappi, and J. L. Dugelay. Multimodal authentication on smartphones: Combining iris and sensor recognition for a double check of user identity. *Pattern Recognition Letters*, 3:34–40, 2015.
- [20] Z. J. Geradts, J. Bijhold, M. Kieft, K. Kurosawa, and K. Kuroki. Methods for identification of images acquired with digital cameras. *Proc. SPIE 4232, Enabling Technolo*gies for Law Enforcement and Security, 2001.
- [21] T. Gloe, M. Kirchner, A. Winkler, and R. Böhme. Can we trust digital image forensics? In *Proceedings of the ACM International Multimedia Conference and Exhibition*, pages 78–86. 01 2007.
- [22] M. Goljan, J. Fridrich, and M. Chen. Defending against fingerprint-copy attack in sensor-based camera identification. *IEEE Transactions on Information Forensics and Security*, 6(1):227–236, March 2011.
- [23] M. Goljan, J. J. Fridrich, and M. Chen. Sensor noise camera identification: countering counter-forensics. In *Media Forensics and Security*, 2010.
- [24] N. Kalka, N. Bartlow, B. Cukic, and A. Ross. A preliminary study on identifying sensors from iris images. In *IEEE Con*ference on Computer Vision and Pattern Recognition Workshops (CVPRW), pages 50–56, June 2015.
- [25] X. Kang, Y. Li, Z. Qu, and J. Huang. Enhancing source camera identification performance with a camera reference phase sensor pattern noise. *IEEE Transactions on Informa*tion Forensics and Security, 7(2):393–402, April 2012.
- [26] C. Kauba, L. Debiasi, and A. Uhl. Identifying the origin of iris images based on fusion of local image descriptors and PRNU based techniques. In 3rd International Joint Conference on Biometrics (IJCB), October 2017.
- [27] B. Levy. Review of "Digital image forensics: There is more to a picture than meets the eye" by Husrev Taha Sencar and Nasir Memon (Editors). volume 4, page 17. 2013.
- [28] C. T. Li. Source camera identification using enhanced sensor pattern noise. *IEEE Transactions on Information Forensics* and Security, 5(2):280–287, June 2010.
- [29] C.-T. Li, C.-Y. Chang, and Y. Li. On the repudiability of device identification and image integrity verification using sensor pattern noise. In D. Weerasinghe, editor, *Information Security and Digital Forensics*, pages 19–25, Berlin, Heidelberg, 2010. Springer Berlin Heidelberg.

- [30] X. Lin and C. T. Li. Enhancing sensor pattern noise via filtering distortion removal. *IEEE Signal Processing Letters*, 23(3):381–385, March 2016.
- [31] X. Lin and C. T. Li. Preprocessing reference sensor pattern noise via spectrum equalization. *IEEE Transactions on In*formation Forensics and Security, 11(1):126–140, Jan 2016.
- [32] J. Lukas, J. Fridrich, and M. Goljan. Digital camera identification from sensor pattern noise. *IEEE Transactions on Information Forensics and Security*, 1(2):205–214, June 2006.
- [33] F. Marra, G. Poggi, C. Sansone, and L. Verdoliva. A deep learning approach for iris sensor model identification. *Pattern Recognition Letters*, 2017.
- [34] V. Mirjalili and A. Ross. Soft biometric privacy: Retaining biometric utility of face images while perturbing gender. In *IEEE International Joint Conference on Biometrics (IJCB)*, pages 564–573, Oct 2017.

- [35] S. Samaras, V. Mygdalis, and I. Pitas. Robustness in blind camera identification. In 23rd International Conference on Pattern Recognition (ICPR), pages 3874–3879, Dec 2016.
- [36] S. A. C. Schuckers, N. A. Schmid, A. Abhyankar, V. Dorairaj, C. K. Boyce, and L. A. Hornak. On techniques for angle compensation in nonideal iris recognition. *IEEE Transactions on Systems, Man, and Cybernetics, Part B (Cybernetics)*, 37(5):1176–1190, Oct 2007.
- [37] A. Uhl and Y. Höller. Iris-sensor authentication using camera PRNU fingerprints. In 5th IAPR International Conference on Biometrics (ICB), pages 230–237, March 2012.
- [38] L. J. G. Villalba, A. L. S. Orozco, J. R. Corripio, and J. Hernandez-Castro. A PRNU-based counter-forensic method to manipulate smartphone image source identification techniques. *Future Generation Computer Systems*, 76:418 – 427, 2017.